

Regulation of atmospheric CO₂ by deep-sea sediments in an Earth system model

Andy Ridgwell^{1,2} and J. C. Hargreaves³

Received 20 May 2006; revised 13 January 2007; accepted 6 February 2007; published 4 May 2007.

[1] We have extended the GENIE-1 Earth system model to include a representation of sedimentary stratigraphy and the preservation of biogenic carbonates delivered to the ocean floor. This has enabled us to take a novel approach in diagnosing modern marine carbon cycling: assimilating observation of the calcium carbonate (CaCO₃) content of deep-sea sediments with an ensemble Kalman filter. The resulting calibrated model predicts a mean surface sediment content (32.5 wt%) close to the observed value (34.8 wt%), and a global burial rate of CaCO₃ in deep sea sediments of 0.121 PgC yr⁻¹, in line with recent budget estimates of 0.10–0.14 PgC yr⁻¹. We employ the GENIE-1 model in quantifying the multimillennial-scale fate of fossil fuel CO₂ emitted to the atmosphere. In the absence of any interaction between ocean and sediments, an equilibrium partitioning of CO₂ is reached within ~1000 years of emissions ceasing, with 34% (645 ppm) remaining in the atmosphere out of a total fossil fuel burn of 4173 PgC. An additional 12% of CO₂ emissions (223 ppm) are sequestered as bicarbonate ions (HCO₃⁻) by reaction with deep-sea carbonates (“seafloor CaCO₃ neutralization”) on a timescale of ~1.7 ka. Excess of carbonate weathering on land over deep-sea burial results in a further net transformation of 14% of CO₂ emissions (261 ppm) into HCO₃⁻ (“terrestrial CaCO₃ neutralization”) on a timescale of ~8.3 ka. We have also assessed the importance of a changing climate in modulating the stabilization of atmospheric CO₂ through ocean-sediment interaction. Increased ocean stratification suppresses particulate organic carbon export, which in turn enhances seafloor CaCO₃ preservation. The resulting reduction in the sequestration of fossil fuel CO₂ represents a new positive feedback on millennial-scale climate change.

Citation: Ridgwell, A., and J. C. Hargreaves (2007), Regulation of atmospheric CO₂ by deep-sea sediments in an Earth system model, *Global Biogeochem. Cycles*, 21, GB2008, doi:10.1029/2006GB002764.

1. Introduction

[2] The sediments of the deep-sea are fundamental to how the concentration of CO₂ in the atmosphere is regulated on timescales of thousands to tens of thousands of years (see *Ridgwell and Zeebe* [2005] for a review). This role arises because the rate of dissolution of biogenic minerals deposited to marine sediments, particularly calcium carbonate (CaCO₃) and opal (amorphous hydrated silica), is responsive to changes in the overlying ocean geochemistry. By inducing a change in the dissolution flux of solutes out of the sediments, the oceanic concentrations of carbonate ions (CO₃²⁻) and silicic acid (H₄SiO₄) are buffered against perturbation.

[3] Spatial and temporal variability in the properties of sediments accumulating at the ocean floor also record important information about the state of ocean biogeochemical cycling. For instance, observed distributions of surface sedimentary properties, particularly the major solid constituents CaCO₃ and opal, reflect ecological patterns among marine plankton at the ocean surface as well as the depth of the seafloor and geochemistry of the abyssal ocean. Sediment property data thus provides a means of validating models of modern ocean carbon cycling. Deep-sea sediments also contain an invaluable archive of past changes in biogeochemical cycling, recorded as down core variations in sediment solid composition, trace metals, and isotopic properties. These variations can be interpreted by means of the forward modeling of sediment mass balance and accumulation in synthetic sediment cores [*Heinze*, 2001; *Ridgwell*, 2001, 2006] (also A. Ridgwell, Dissolution response of marine carbonates to massive CO₂ release: Implications for the interpretation of the PETM, submitted to *Paleoceanography*, 2007) (hereinafter referred to as Ridgwell, submitted manuscript, 2007).

[4] To be able to explicitly simulate the role of the marine carbonate cycle in regulating atmospheric CO₂ on multi-

¹Department of Earth and Ocean Sciences, University of British Columbia, Vancouver, British Columbia, Canada.

²Now at School of Geographical Sciences, University of Bristol, Bristol, UK.

³Frontier Research Center for Global Change, Yokohama, Japan.

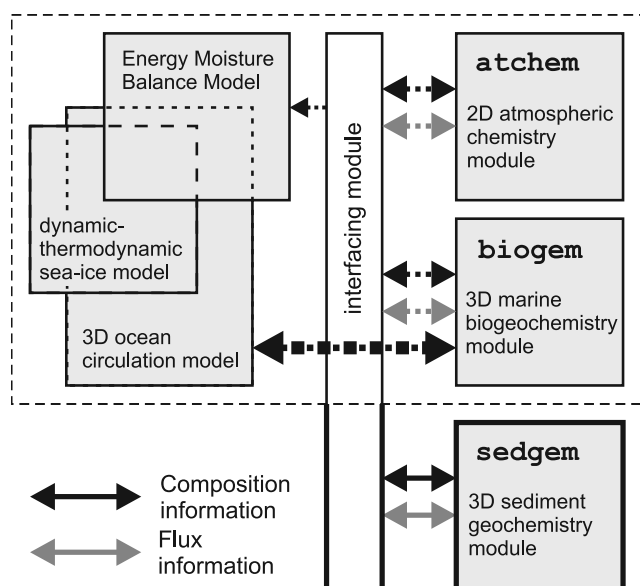


Figure 1. Schematic of the relationship between the different model components comprising the GENIE-1 model. Outlined in bold is the sediment module SEDGEM described in this paper, while the ocean carbon cycle + climate model [Ridgwell *et al.*, 2007] is delineated by a dashed box.

millennial timescales, as well as providing a means of validating model biogeochemical cycling and mechanistically interpreting the paleoceanographic record, we have extended the capabilities of the coupled ocean carbon cycle + climate “Grid ENabled Integrated Earth system model” (GENIE-1) by adding a representation of the preservation and burial of calcium carbonate (CaCO₃) in deep-sea sediments. The GENIE-1 model is based on the fast climate model of Edwards and Marsh [2005], featuring a reduced physics (frictional geostrophic) 3-D ocean circulation model coupled to a 2-D energy-moisture balance model (EMBM) of the atmosphere and a dynamic-thermodynamic sea-ice model and contains a representation of marine carbon cycling with a simple single nutrient (phosphate) control on biological productivity, calibrated against observational data sets of ocean geochemistry [Ridgwell *et al.*, 2007].

2. Sediment Model Description

2.1. Overview

[5] The sediment geochemistry model (SEDGEM) has a relationship to the other biogeochemical and climate components of the GENIE-1 Earth system model as illustrated in Figure 1. In brief, the sediment model is based on work by Ridgwell [2001]: a single surface layer underlain by a stack of sediment storage layers. Here the surface layer is nominally assigned a thickness of 5 cm and represents the upper zone of the sediments in which mixing effectively homogenizes solid composition and where carbonate dissolution primarily takes place [e.g., Archer *et al.*, 1989; Emerson and Bender, 1981]. The storage layers in the

sediment stack are all 1 cm thick, with the exception of the layer lying at the top of the stack which varies in thickness (between 0 and 1 cm) depending on net sediment accumulation or dissolution. The sediment stack thus grows or shrinks from the top, depending on the sign of the mass balance in the surface layer, which remains at constant thickness (5 cm). Finally, a diffusive-like transfer is prescribed between adjacent layers to provide a vertical mixing of solids: bioturbation (see Ridgwell, submitted manuscript, 2007).

[6] Here we consider the solid sedimentary components (tracers) to be CaCO₃ (as the calcite polymorph) and detrital material. The detrital tracer implicitly includes opal, which we do not explicitly model, in addition to refractory materials derived from aeolian deposition at the ocean surface and transported off of the continental slopes and shelves. The detrital flux to the sediments is imposed as a boundary condition as described in section 2.3. We assume that all organic matter is entirely remineralized in the surface sediments of the deep sea and so omit organic matter as an explicit component of accumulating sediments.

[7] A variety of properties of bulk carbonate are included in SEDGEM. The mean $\delta^{13}\text{C}$ of CaCO₃ in each sediment layer is updated according to mixing and advective exchange between sediment layers. For the surface layer, mean carbonate $\delta^{13}\text{C}$ is also updated according to the mass and isotopic composition of CaCO₃ rain input and dissolution loss. The radiocarbon content (and $\delta^{14}\text{C}$) of CaCO₃ is treated identically, except that it decays with a half-life of 5730 years [Stuiver and Polach, 1977]. We also tag carbonate newly deposited to the sediments with the current model time, equivalent to calendar years before present. This allows us to plot down core variability in simulated sediment properties as a function of age, which greatly facilitates comparison between synthetic and observed paleoceanographic records (Ridgwell, submitted manuscript, 2007).

[8] To maximize the overall computational speed of the GENIE-1 model, we chose a SEDGEM time step 20 times longer than the time step length of 0.05 years taken by the ocean biogeochemistry module (BIOGEM) [Ridgwell *et al.*, 2007]. This asynchronicity is handled by an interfacing module (Figure 1) which integrates the rain flux to the sediments over the one year of the SEDGEM time step before being added to the surface sediment layer. In the opposite direction, the sediment dissolution flux to the ocean is assumed constant over the same interval (1 year). The interfacing module is also capable of simple transformations between model grids, allowing us to use a finer grid (72 × 72) for the sediments than is provided for by the ocean circulation model (36 × 36) (see section 4).

[9] A separate sediment module comprising surface layer and stack is assigned to each wet grid point in the ocean circulation model. The underlying sedimentary diagenesis model employed to calculate carbonate dissolution is the oxic-only model of Archer [1991, 1996]. Because this does not account for suboxic and anoxic respiration of organic carbon, it is not well suited to the elevated particle flux rates and sedimentation rates characterizing shallow water environments for which a more involved and computationally

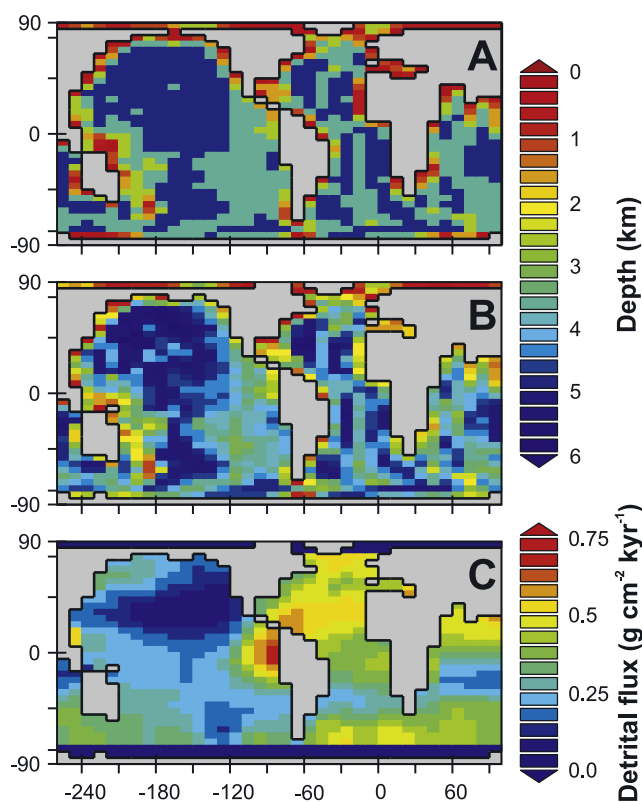


Figure 2. Sedimentary boundary conditions in GENIE-1. (a) The bathymetry of the ocean circulation model [Edwards and Marsh, 2005]. (b) Bathymetry derived from modern topographic data (ETOPO2: 2-minute gridded global relief data, 2001, <http://www.ngdc.noaa.gov/mgg/fliers/01mkg04.html>) and used by the sediment module for calculating hydrostatic pressure. No sediments are simulated immediately underlying (or lying within) the shallowest ocean level (≤ 175 m water depth) and are represented by the same grey fill as the continental area. (c) Global distribution of non-carbonate (opal and clay) accumulation rates in the modern ocean, re-gridded from Archer [1996].

expensive redox diagenesis model such as “Muds” [Archer *et al.*, 2002] would be required. We therefore do not attempt to calculate carbonate content where the surface ocean layer in the model directly overlies the sediments, i.e., where ocean depth is ≤ 175 m. Each sediment module is driven by particulate settling fluxes as well as ambient temperature and salinity, and the concentrations of biogeochemical tracers (DIC, ALK, PO₄, etc.) in the overlying ocean.

[10] We calculate the hydrostatic pressure at each SEDGEM grid point from global bathymetric data (ETOPO2: 2-minute gridded global relief data, 2001, <http://www.ngdc.noaa.gov/mgg/fliers/01mkg04.html>) (Figure 2b) rather than taking it directly from the depths resolved by the ocean circulation model (Figure 2a). We do this because the stability of calcite and thus the degree of carbonate preservation is highly sensitive to water depth

[Archer, 1996]. In contrast, CaCO₃ and POC settling fluxes recorded in sediment traps appear to be relatively independent of depth below about 2000 m in the water column. Thus away from the continental shelves and slopes the difference in particulate rain rates measured at the respective depths defined by the two bathymetric grids (Figures 2a and 2b) is rather less important to the calculation of CaCO₃ preservation than the corresponding differences in hydrostatic pressure. An alternative might be to double the number of depths levels in the ocean circulation model from 8 to 16 [Ridgwell *et al.*, 2007], thereby improving the resolution of both hydrostatic pressure and rain rates but with a twofold computational penalty.

2.2. Calculation of Carbonate Dissolution

[11] In this paper we adopt a look-up table approach for the efficient encapsulation of diagenetic behavior in SEDGEM following Ridgwell [2001], in which the dissolution flux is obtained through linear interpolation on a regular multidimensional grid of precalculated values. The look-up table values themselves are calculated using the oxic-only model of Archer [1991]. The calculated CaCO₃ dissolution flux is used to update the surface sediment mass balance, with newly deposited CaCO₃ preferentially subject to dissolution over material already present in the surface layer: the interface model for the locus of carbonate of dissolution [Oxburgh and Broecker, 1993].

2.3. Ocean-Sediment System Configuration and Spinup

[12] To calculate steady state sediment composition we configure the model as a “closed” system, i.e., one in which there is no gain of solutes to the ocean from weathering or losses through burial of CaCO₃. To speed up this calculation, we minimize the residence time of CaCO₃ in surface sediments by reducing the surface mixed layer thickness in SEDGEM from 5 cm to 1 cm, and set the scaling mixing coefficient for bioturbation to zero. The parameter values controlling marine carbon cycling in GENIE-1 are initially taken from a previous eight-parameter calibration of the model made against ocean geochemical observations [Ridgwell *et al.*, 2007] (configuration “PA_8” in Table 1) and provided as auxiliary material¹. We integrate the model for 25 ka, starting with deep-sea sediment composition set to 0 wt% CaCO₃. A detrital flux is applied to the ocean surface, sinking instantaneously and without alteration to the underlying sediments. This is derived from the gridded noncarbonate accumulation map of Archer [1996] which includes contributions from opal as well as dust and material from nonaeolian (e.g., continental shelf) sources. When transformed to the 2-D (36 × 36) SEDGEM model grid the applied flux has a spatial distribution as shown in Figure 2c. This is held constant with time.

[13] The resulting surface sediment layer distribution of CaCO₃ is shown in Figure 3c. Mean sedimentary CaCO₃ content is 40.3 wt%, compared to a data-based value of 34.8 wt%. Although the sedimentary CaCO₃ dissolution

¹Auxiliary materials are available at <ftp://ftp.agu.org/apend/gb/2006gb002764>.

Table 1. Sensitivity of Atmospheric CO₂ Response to Alternative Calibrations of the GENIE-1 Model

EnKF ID	Mean CaCO ₃ , wt%	CaCO ₃ Burial, PgC yr ⁻¹	Peak CO ₂ , ppm	Year 3000 CO ₂ , ppm	Year 10,000 CO ₂ , ppm	Year 50,000 CO ₂ , ppm	Summary of Model Configuration
PA_8	40.3	0.179	1315	918	516	423	8-parameter PO ₄ + ALK assimilation 36 × 36 grid
PAC_8	32.4	0.121	1311	914	557	423	8-parameter PO ₄ + ALK + CaCO ₃ assimilation, 36 × 36 grid
PAC_8	33.1	0.121	1311	918	569	424	8-parameter PO ₄ + ALK + CaCO ₃ assimilation, 72 × 72 grid
PAC_10	38.4	0.153	1311	911	527	422	10-parameter PO ₄ + ALK + CaCO ₃ assimilation, 36 × 36 grid

flux (43 Tmol C yr⁻¹) falls slightly outside of previous model-based estimates (25–40 Tmol C yr⁻¹ [Archer, 1996]), the global mean carbonate preservation efficiency of 25.8% is consistent with the 20–30% range estimated by Archer [1996]. Possible reasons for an overprediction of CaCO₃ abundance are that the relatively weak gradients of PO₄³⁻ and ALK in the deep ocean are insufficient constraints on the fluxes of POC and CaCO₃ to the ocean floor, or that a general bias exists toward high CaCO₃ rain rates and/or low POC fluxes in our representation of marine carbon cycling.

[14] An additional potential source of bias in the model simulation of deep-sea sedimentary CaCO₃ preservation concerns the configuration of the model as a closed system, with no weathering input or burial loss. We exclude this as the cause of the carbonate abundance overprediction by now allowing removal of DIC and ALK from the ocean according to CaCO₃ burial and prescribe a global carbonate weathering flux of 0.179 PgC yr⁻¹ to balance this. After a further 10 ka of open system integration we find that the mean sedimentary composition changes by <0.1 wt% CaCO₃ suggesting that configuration as a closed system is not an important source of error. The reason why the closed system produces a reasonable approximation of (steady state) sediment composition in an open system is that most (~70–80%) of the CaCO₃ rain flux reaching the sediment surface dissolves and is returned to the ocean anyway, so that the impact on bottom water carbonate chemistry and CaCO₃ preservation of imposing a 100% return to create a closed system is relatively small.

3. Data Assimilation and Calibration of Ocean-Sediment Carbon Cycling

[15] In this paper we address the potential for using observations of sediment composition to better constrain the modern marine carbon cycle. We use the same ensemble Kalman filter (EnKF) method [Annan *et al.*, 2005; Hargreaves *et al.*, 2004] for calibrating the model parameters as employed by Ridgwell *et al.* [2007]. The difference here is that as well as 3-D data sets of dissolved phosphate (PO₄) and alkalinity (ALK) distributions in the ocean, we also include a 2-D data field, describing the observed distribution of wt% CaCO₃ in the surface sediments of the deep sea (Figure 3b). In the assimilation calculation the data are normalized so that each grid point for which there is some information takes approximately equal weight in the cost function. Therefore, in the parameter calibration calculation, the overall effect of the 3-D PO₄ and ALK data fields is stronger than that of the 2-D CaCO₃ field. Of the eight parameters that we calibrate (see auxiliary material), we

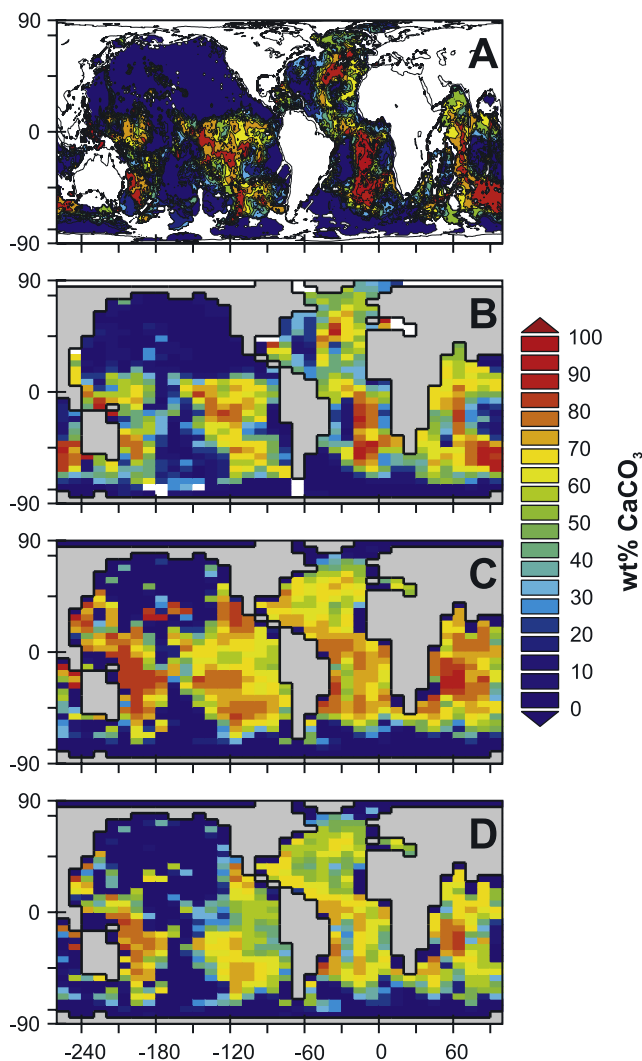


Figure 3. Observed and model-predicted sedimentary CaCO₃ content. (a) Observed distribution of sediment surface wt% CaCO₃ interpolated on a 1° × 1° grid [Archer, 1996]. Areas with no data coverage, such as parts of the Southern Ocean and many of the continental margins, are left blank. (b) Observed wt% CaCO₃ data transformed onto the SEDGEM grid. Grid points for which none of the 1° × 1° data of Archer [1996] falls within a grid cell are left blank (white). (c) Sediment composition predicted by GENIE-1 calibrated against ocean PO₄ and alkalinity distributions only [Ridgwell *et al.*, 2007] (‘PA_8’). (d) Sediment composition predicted by assimilation of observed core top wt% CaCO₃ (Figure 3b) in addition to ocean PO₄ and alkalinity distributions (‘PAC_8’).

modify our prior ranges for the parameters η and $r_0^{\text{CaCO}_3:\text{POC}}$ to reflect the range found in a recent data synthesis of acidification experiments carried out on marine calcifiers [Ridgwell *et al.*, 2006]. In our formulation of carbonate export, $r_0^{\text{CaCO}_3:\text{POC}}$ is a spatially uniform scalar while η controls the degree of nonlinearity between calcification rate and local ambient saturation (Ω) [see Ridgwell *et al.*, 2007],

$$\gamma = (\Omega - 1)^\eta \quad \Omega > 1.0 \quad (1a)$$

$$\gamma = 0.0 \quad \Omega \leq 1.0. \quad (1b)$$

[16] The product of the modifier γ and $r_0^{\text{CaCO}_3:\text{POC}}$ gives the local CaCO₃:POC export rain ratio. Because the equilibrium time of the sediment model is several times that of ocean biogeochemistry, the run time for each model iteration between applications of the EnKF is increased from 100 to 500 years. The EnKF method is well converged after each ensemble member has been run for a total of 25,000 years. This eight-parameter calibration is labeled “PAC_8” (Table 1). Although we will use the PAC_8 calibration in the remainder of this paper in quantifying the long-term fate of fossil fuel CO₂, we have also explored the calibration of some alternative configurations of the model.

[17] In our previous assimilation involving ocean-only geochemical data (PO₄ and ALK) [Ridgwell *et al.*, 2007], fluxes of particulate organic carbon (POC) and CaCO₃ to the deep ocean were close to zero when we tried calibrating two additional parameters controlling deep remineralization length scales of POC and CaCO₃ in a double exponential formulation [Andersson *et al.*, 2004; Lutz *et al.*, 2002]. In this parameterization, the particulate flux measured at depth z in the ocean, F_z is described by

$$F_z = F_{z=h_e} \cdot \left((1-r) \cdot \exp\left(\frac{z_{h_e}-z}{l_2}\right) + r \cdot \exp\left(\frac{z_{h_e}-z}{l_1}\right) \right), \quad (2)$$

where l_1^{POC} and l_2^{POC} are the two length scales of remineralization, r^{POC} is the partitioning of the two fractions of exported particulate matter, and h_e is the depth at which export is measured, equal to the surface layer depth of 175 m. By substituting ∞ for the second length scale (l_2) the equation becomes identical to that used previously in the 8 parameter calibration [Ridgwell *et al.*, 2007]. This would be fully justified if the second fraction of the organic matter should sink quickly and/or remineralize slowly enough that decay is essentially zero [Lutz *et al.*, 2002]. We tested whether the addition of observations of sediment composition in the EnKF might allow us to quantify the remineralization length scale of biogenic material in the deep ocean (“PAC_10”). Although with the inclusion of the new data constraint, a stable solution to the calibration of 10 parameters was obtained, the two new parameters do not change much from the assumed prior ranges (see auxiliary material). In addition, when adopting these prior ranges, the overall cost was not significantly improved but the global mean and distribution of wt% CaCO₃ in the sediments was degraded. This may reflect the simplicity of

the remineralization parameterizations we have adopted or that the strong hydrostatic pressure control on the rate of dissolution of CaCO₃ obscures the effect of relatively subtle decreases in settling flux with depth in the abyssal ocean. Alternatively, one or more of our prior assumptions¹ may prevent the EnKF from achieving an improved CaCO₃ solution. A more rigorous search for the optimal remineralization length scales is beyond the scope of this current paper.

[18] We have also tried different possible configurations of the sediment model SEDGEM in a series of eight-parameter calibrations. For instance, we have tested substituting the data-based noncarbonate accumulation flux (Figure 2c) with a spatially uniform detrital flux of 0.18 g cm⁻² ka⁻¹ [Archer *et al.*, 1998] or atmospheric GCM simulated aeolian deposition to the surface ocean. We also tested the effect of using the ocean model grid (Figure 2a) to calculate hydrostatic pressure rather than observed bathymetry (Figure 2b). All combinations of these alternative assumptions led to a poorer simulation of the wt% distribution of CaCO₃ in the sediments (not shown). The results of these assimilations will not be considered further here.

[19] Finally, it should be recognized that because of large uncertainties in model structure, meaning that the model is known a priori to be a far from perfect model, using the full ensemble results to provide probabilistic estimates of model variables or parameters would not be a valid approach, as discussed by Ridgwell *et al.* [2007]. For the results and applications in this paper we therefore show only the results using the ensemble means of the eight calibrated parameters. We explore the application of the full 54-member ensemble in sensitivity (as opposed to probabilistic) analysis of fossil fuel CO₂ uptake by the ocean elsewhere [Ridgwell *et al.*, 2006].

4. Present-Day Global Carbonate Cycling

[20] The distribution of carbonates in the surface sediments predicted by the GENIE-1 model calibrated against ocean PO₄ and ALK and sedimentary wt% CaCO₃ is shown in Figure 3, and is markedly closer to the sediment observations than with the previous calibration with PO₄ and ALK only. Global mean surface sediment CaCO₃ content is now 32.5 wt% and much closer to the observational-based estimate of 34.8 wt%; although this data-based mean is probably something of an overestimate because the data gaps are predominantly located in carbonate poor regions. The improvement in wt% CaCO₃ afforded by the addition of 2-D sediment data in the EnKF resulted in only a very slight degradation in the quality of alkalinity and phosphate fields compared to observations, less than 1% increase in the mean square difference between the data and the model fields compared to that presented by Ridgwell *et al.* [2007]. Thus assimilation of sediment composition data has provided constraints on the operation of marine carbon cycling that ocean geochemical observations alone could not provide, at least in the context of the resolution and parameterizations of our model.

[21] Model-predicted global export production of CaCO₃ is 1.26 PgC yr⁻¹ is very close to the “preferred estimate” of

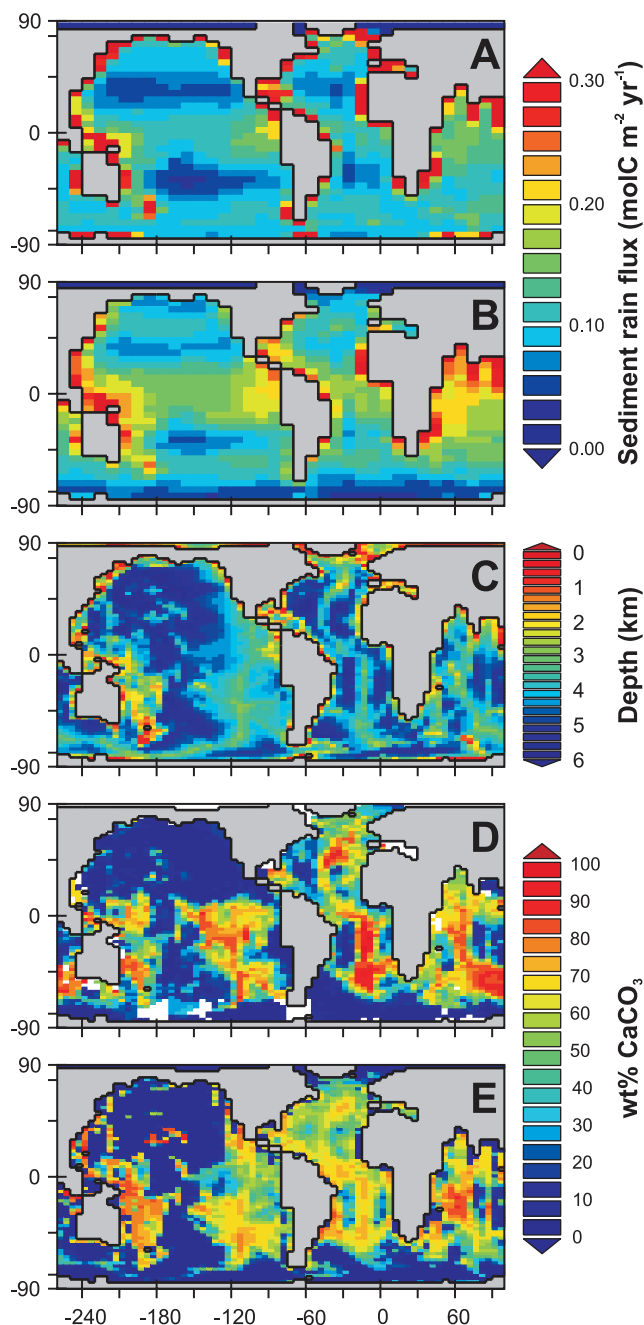


Figure 4. Subgridding of deep-sea sediments in GENIE-1. (a, b) Rain flux of particulate organic carbon and carbonate carbon, respectively, to the sediment surface. The rain fluxes are calculated on the (36×36) ocean model grid using the PAC_8 configuration. (c, d) Observed topography (ETOPO2: 2-minute gridded global relief data, 2001) and sediment composition [Archer, 1996], transformed to a 72×72 equal area grid. (e) Predicted core top wt% CaCO₃ distribution on a 72×72 equal area grid.

1.14 PgC yr^{-1} diagnosed by Jin *et al.* [2006] from global nutrient and alkalinity distributions. The CaCO₃ rain flux to the sediments of the open ocean ($>175 \text{ m}$ water depth in the model) is 0.64 PgC yr^{-1} and is associated with a flux of

particulate organic carbon (POC) of 0.87 PgC yr^{-1} . Of the CaCO₃ rain to the sediment surface, $0.121 \text{ PgC yr}^{-1}$ is preserved and buried, a value that lies at the centre of recent global carbonate budget estimates of $0.1\text{--}0.14 \text{ PgC yr}^{-1}$ [Feely *et al.*, 2004].

[22] Some areas of model-data mismatch still remain, such as the margin upwelling settings of the subtropical ($\sim 10^\circ\text{N}\text{--}25^\circ\text{N}$ and $\sim 10^\circ\text{S}\text{--}35^\circ\text{S}$) Eastern Pacific, where CaCO₃ incorrectly accumulates in the model. This could be due to overprediction of the importance of calcifiers and biogenic CaCO₃ production there. While the “C” shape of high CaCO₃ in the Western and central Indian Ocean is reasonably reproduced, the Eastern margin around 40°S is underpredicted compared to observations. In general, there is also a tendency toward insufficient contrast between topographically controlled wt% CaCO₃ highs and lows, which is particularly apparent in the Atlantic. This could reflect a bias toward an organic carbon control of CaCO₃ dissolution in deep-sea sediments compared to bottom water undersaturation, originating either from the underlying representation of sedimentary diagenesis [Archer, 1991], its look-up table encapsulation, and/or from the model-predicted POC rain flux to the ocean floor. That the difference between ambient $[\text{CO}_3^{2-}]$ and that required for thermodynamic saturation with respect to calcite (ΔCO_3^{2-}) in the model is generally $\sim 10\text{--}20 \mu\text{mol kg}^{-1}$ higher than we estimate from marine geochemical observations, suggests that dissolution driven by organic carbon metabolism in the sediments is slightly overrepresented. Overall however, our calibrated model compares extremely favorably with the predictions of much higher-resolution 3-D ocean-only biogeochemical models [e.g., Archer *et al.*, 2000; Gehlen *et al.*, 2006; Heinze *et al.*, 1999].

[23] On a scale rather smaller than ocean basins ($<1000 \text{ km}$), the dominant control on the CaCO₃ content of deep-sea sediments is hydrostatic pressure [Archer, 1996]. This is evident in the data-based reconstruction shown in Figure 3a, topographic highs correlate strongly with areas of higher wt% CaCO₃ compared to sediments elsewhere in the same basin and at similar latitudes. In contrast, at the global scale, the large-scale circulation of the ocean and water mass geochemistry dominates [Ridgwell and Zeebe, 2005].

[24] We can capture the hydrostatic control at a finer scale than is possible at the native resolution of the ocean circulation model (36×36 in this case) by subgridding the sediments. We chose a simple factor of two in both latitude and longitude for the SEDGEM sediment module, giving a 72×72 equal area grid. The bathymetry associated with this grid is shown in Figure 4c. We justify increasing the resolution of the sediment model independently of the ocean model because away from the continental margins, the rain fluxes of biogenic material to the sediments vary proportionally less with distance (Figures 4a and 4b) than does depth (Figures 2b and 4c). We do not run the entire GENIE-1 model at 72×72 resolution because this would increase run time by a factor of ~ 8 , making access to the timescales and questions of interest problematic.

[25] The predicted distribution of sedimentary carbonate with a twofold subgridding of the sediments is shown in Figure 4e. Note that the model has not been recalibrated; the

parameter values are the same as discussed in section 4 (“PAC_8”) and listed in auxiliary material. We now capture much more of the observed variability in sediment composition (Figure 4d), although the same broad-scale model-data mismatches remain. The mean sedimentary CaCO₃ content of deep-sea sediments (33.3 wt%) and global deep-sea carbonate sink (0.121 PgC yr⁻¹) are little changed.

[26] Subgridding is likely to be particularly advantageous where transects of cores from a relatively small geographic region are used to reconstruct changes in paleo lysocline depth and one desires to employ an ocean carbon cycle model to formally test hypotheses for these observations but without having to resort to a much higher-resolution (and thus slower) ocean circulation model. In this paper, we do not address any paleoceanographic questions and so employ SEDGEM at 36 × 36 resolution. The 72 × 72 subgridded model is applied elsewhere (Ridgwell, submitted manuscript, 2007).

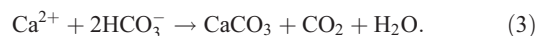
5. Long-Term Fate of Fossil Fuel CO₂

[27] We now quantify the role of ocean-sediment interactions in controlling the long-term fate of fossil fuel CO₂ using our calibrated Earth system model. Our analysis here concerns a single illustrative CO₂ emissions scenario, based on the assumption of all conventional fossil fuel reserves (~4000 PgC) being used up sometime early in the 24th century [Lenton *et al.*, 2006], a figure slightly less than the 5720 PgC total “burn” assumed by Caldeira and Wickett [2003]. The prescribed time-history of the anthropogenic CO₂ flux to the atmosphere is shown in Figure 5a and comprises the following components. From the year 1765 to 2000 the emissions trajectory is deduced consistent with the observed trajectory of atmospheric CO₂ [Enting *et al.*, 1994; Keeling and Whorf, 2004]. Until 2100, emissions follow the IS92a scenario, followed by a linear decline in emissions to use up all “conventional” fossil fuel reserves of circa 4000 GtC [Lenton, 2000]. The predicted CO₂ trajectory implicitly assumes no change in land carbon storage either due to interaction with the terrestrial biosphere (addressed elsewhere [Lenton *et al.*, 2006]) or changes in anthropogenic land use [e.g., Sitch *et al.*, 2005]. Although the GENIE-1 Earth system model can account for feedbacks between CO₂ and climate and between CO₂ and calcification, we initially hold climate constant at its pre-industrial state

[Hargreaves *et al.*, 2004; Ridgwell *et al.*, 2007] and do not allow the CaCO₃:POC export rain ratio to respond to surface ocean acidification; that is, we prescribe a pre-industrial spatial distribution of CaCO₃:POC rain ratio.

[28] We first run the CO₂ emissions experiment with our model in a closed system configuration with no weathering input to the ocean. The loss of DIC and ALK from the ocean due to the burial of CaCO₃ in deep-sea sediments is instead balanced by prescribing an additional solute flux from the sediments equal to the calculated burial rate of CaCO₃. This configuration is analogous to most current 3-D ocean carbon cycle models. The resulting evolution of atmospheric CO₂ is shown in Figure 5b. By the start of the next millennium (year 3000), the ocean has achieved near equilibrium with atmospheric composition, with 1418 PgC of fossil fuel CO₂ remaining in the atmosphere, equivalent to 923 ppm above the pre-industrial concentration of 278 ppm. In this case, the ocean is able to sequester a maximum of 66.3% of the total atmospheric release of 4173 PgC, storing it mainly in the form of bicarbonate ions (HCO₃⁻) (Figure 5c).

[29] The dynamical response of a closed system can be very different from that of an “open” system where there is a continual throughput (i.e., both sources and sinks of a dissolved species to the ocean) [Hotinski *et al.*, 2000]. The preservation of CaCO₃ deposited to deep-sea sediments represents the loss of dissolved inorganic carbon (DIC) and Ca²⁺ and thus alkalinity (ALK) from the ocean,



For the ocean-sediment system to be in steady state, this loss must be balanced primarily by the weathering of carbonates in soils and at exposed rock surfaces,



with a further contribution from the weathering of calcium silicate minerals.

[30] Estimates for the total present-day bicarbonate ion (HCO₃⁻) flux to the ocean vary between 23 and 39 Tmol C yr⁻¹ depending on assumptions about runoff and underlying lithology, as well as the details of the relationship of solute flux to both factors [Gibbs *et al.*, 1999; Munhoven,

Figure 5. The role of ocean-sediment interactions in the sequestration of fossil fuel CO₂. (a) Time-history of the rate of CO₂ emission to the atmosphere prescribed in the model. (b) Predicted trajectory of atmospheric CO₂. The light shaded region indicates the reduction of atmospheric CO₂ that is due to seafloor CaCO₃ neutralization alone ($\Delta\text{CO}_{2(\text{final})}$ seafloor), while the dark shaded region is that due to terrestrial CaCO₃ neutralization alone ($\Delta\text{CO}_{2(\text{final})}$ terrestrial). (c) Evolution of ocean carbonate chemistry: CO_{2(aq)}, HCO₃⁻, and CO₃²⁻, plotted as mean ocean concentrations ($\mu\text{mol kg}^{-1}$). (d) Evolution of global surface sediment composition (wt% CaCO₃). The minimum in sedimentary carbonate content corresponds to the transition of CaCO₃ accumulation (Figure 5e) from net erosion to redeposition and replenishment of the surface sedimentary CaCO₃ reservoir. (e) Model-predicted global accumulation rate of CaCO₃ in deep-sea sediments. The light shaded area under the curve (negative CaCO₃ accumulation rate) represents the net erosion of carbonates previously deposited in deep-sea sediments by the seafloor CaCO₃ neutralization mechanism, while the darker shaded region represents periods having a positive accumulation rate of CaCO₃, but at a rate lower than the supply of bicarbonate to the ocean by carbonate weathering on land (i.e., terrestrial CaCO₃ neutralization). The prescribed terrestrial weathering rate is indicated by the horizontal dashed line, and the transition from net erosion to deposition of CaCO₃ by the horizontal dotted line. (f) Prescribed CaCO₃ flux forcing for the seafloor neutralization only experiment.

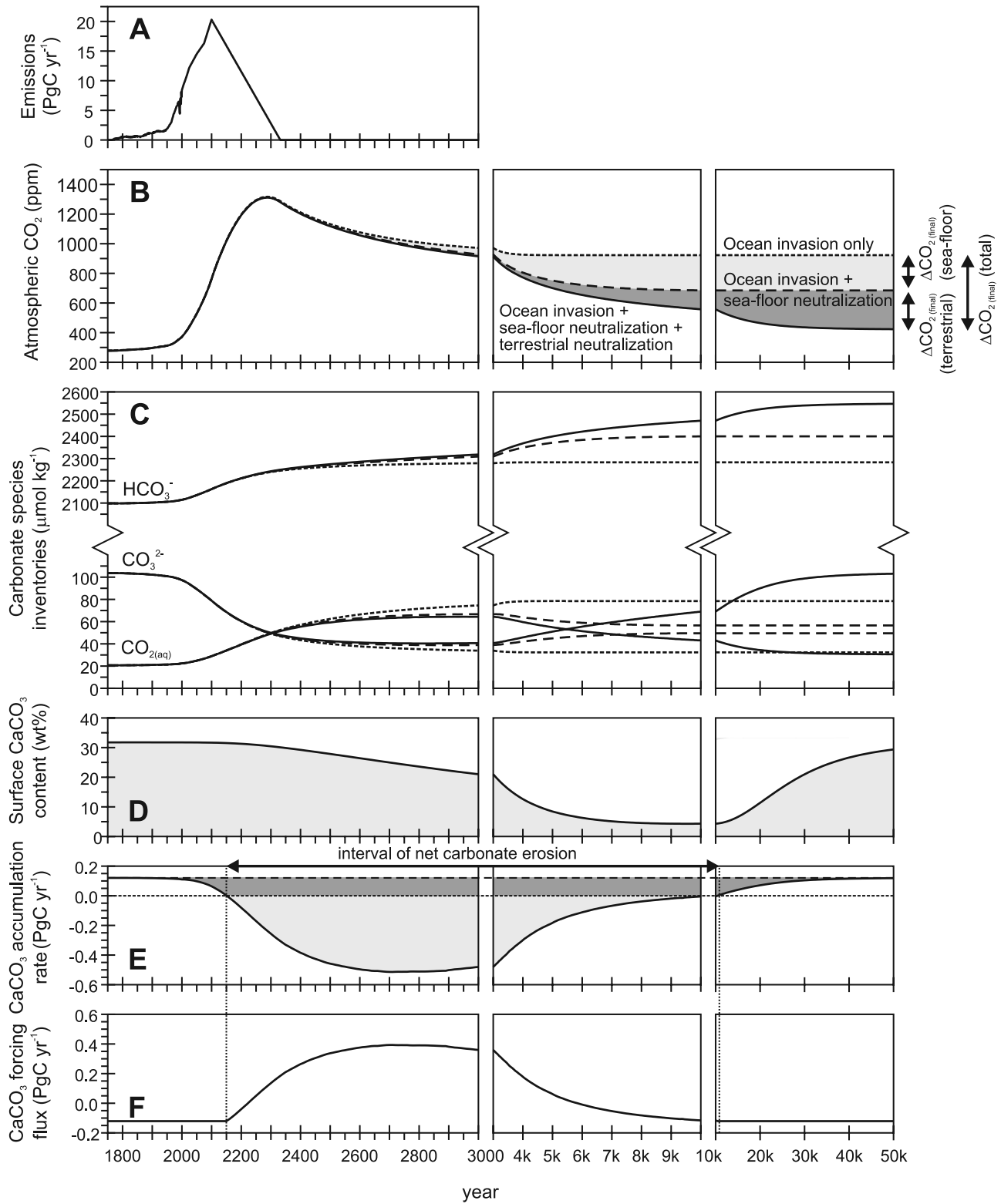


Figure 5

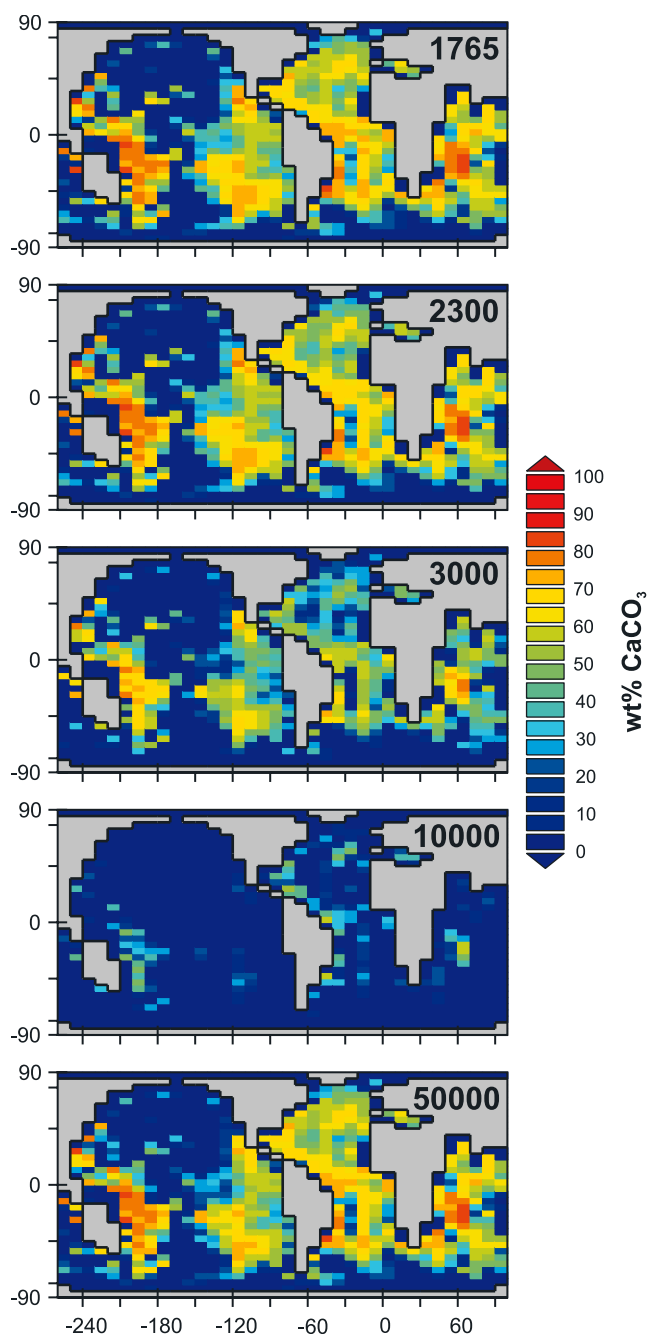


Figure 6. Evolution of sediment surface carbonate content in response to fossil fuel CO₂ release. Time slices shown for the calendar years: 1765, 2300, 3000, 10,000, and 50,000.

2002]. Because two moles of HCO₃⁻ are associated with each mole of CaCO₃ weathered or precipitated, the global sedimentary sink of carbonate must be equal to half the HCO₃⁻ supply flux at steady state, some 12–20 Tmol CaCO₃ yr⁻¹ (= 0.14 – 0.23 PgC yr⁻¹). However, not all carbonate burial takes place in the open ocean – deposition occurs in shallow waters, mainly in the form of carbonate reefs and banks, and is a sink that we do not model here. Although current estimates of modern shallow water CaCO₃

burial place it approximately equal to the deep ocean [Milliman and Drozler, 1996; Vecsei, 2004], there is substantial uncertainty in this. There is also uncertainty as to whether the present-day marine carbonate cycle is at steady state or not [Milliman and Drozler, 1996]. Thus we cannot necessarily assume that the weathering flux required to balance deep-sea CaCO₃ burial is simply equal to say 50% of the global weathering rate. Instead, we ignore the unknown component of weathering that nominally balances shallow water carbonate burial and simply set a weathering flux equal to the CaCO₃ burial rate in deep-sea sediments, 0.121 PgC yr⁻¹, predicted by our previous simulation of sediment composition with the carbon cycle configured as a closed system. That this figure represents >50% of the estimated available solute supply suggests that either our estimate of deep-sea CaCO₃ burial is too high, or more likely, that the global carbonate cycle is not at steady state (i.e., the sum of CaCO₃ sinks exceeds the global weathering input to the modern ocean). It should be noted that particulate organic carbon reaching the sediments is assumed completely remineralized, although CO_{2(aq)} released by remineralization within the sediments is available for driving carbonate dissolution [Archer, 1991]. Thus, unlike global carbonate cycling in the model, the cycle of organic matter and associated nutrients (PO₄) is closed.

[31] We now spin up the model for 50 ka with GENIE-1 configured with an open carbonate cycle as described above, reset the surface sediment layer thickness to 5 cm, and turn bioturbational mixing back on. This time interval is necessary for the open system to approach a steady state balance between inputs (weathering) and outputs (sedimentary burial) as well as to accumulate a sufficient depth of calcareous sediments for subsequent CO₂ driven erosion. We then rerun the fossil fuel CO₂ emissions experiments.

[32] The long-term (>1000 year) evolution of atmospheric CO₂ (Figure 5b) is markedly different in an open system in which the carbonate chemistry of the ocean adjusts through interaction with carbonates deposited to deep-sea sediments. The timescale of CO₂ drawdown is much longer, and the “eventual” (assumed, year 50,000) anthropogenic CO₂ storage by the ocean now represents 92.4% of the total release. Erosion and progressive net dissolution of previously carbonate rich sediments occurs (Figures 5d and 6), and because the rate of burial of CaCO₃ is reduced there is also a net accumulation of the products of continental weathering in the ocean. These two effects are responsible for the additional atmospheric CO₂ drawdown and sequestration by converting CO₂ → HCO₃⁻ compared to by ocean invasion alone. Note that weathering rates are held constant in this experiment, and the ultimate CO₂ sequestration mechanism, silicate weathering is not represented.

5.1. Characterizing the Components of Ocean-Sediment Interaction

[33] The overall buffering of ocean chemistry and atmospheric CO₂ (Figure 5b) by changes induced in the preservation of CaCO₃ in deep-sea sediments is known as “carbonate compensation” [Broecker and Peng, 1987] and represents a key regulatory mechanism in the modern global carbon cycle on timescales of 5–10 ka. The response

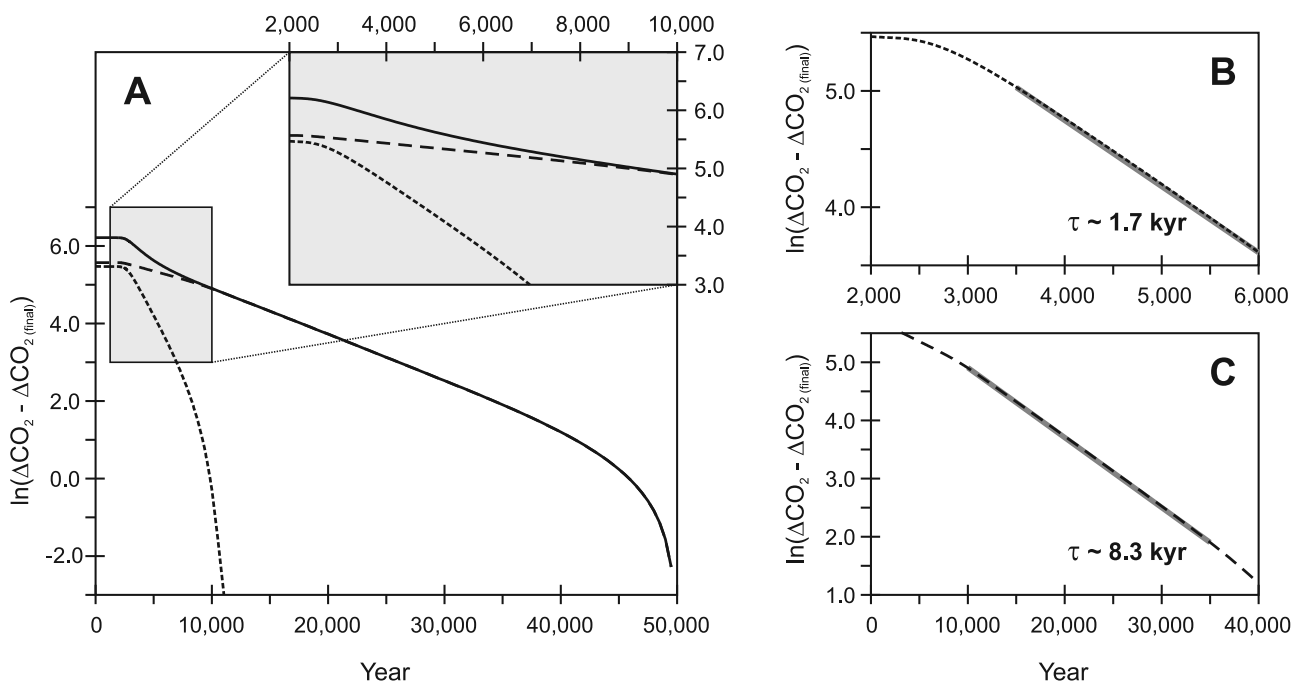


Figure 7. Analysis of the e -folding timescales of ocean-sediment buffering of atmospheric CO₂. (a) The solid line represents the combined contribution of sea floor and terrestrial CaCO₃ neutralization to the removal of fossil fuel CO₂ from the atmosphere. ΔCO_2 is the change in atmosphere CO₂ due to ocean-sediment interactions (ppm), and $\Delta\text{CO}_{2(\text{final})}$ is the maximum CO₂ drawdown, assuming that steady state is approximately attained by the year 50,000. This can be thought of as the combined CO₂ difference of the light grey and dark grey regions in Figure 5b subtracted from their maximum (year 50,000) contribution. Also shown are the contributions to the removal of fossil fuel CO₂ from sea floor (short-dashed line) and terrestrial (long-dashed line) CaCO₃ neutralization. (b) Determination of the e -folding time of atmospheric CO₂ adjusts owing to sea floor CaCO₃ neutralization. The interval over which the e -folding time is calculated is highlighted by a thick grey line. (c) Determination of the e -folding time of atmospheric CO₂ adjusts due to terrestrial CaCO₃ neutralization.

of atmospheric CO₂ to ocean-sediment interaction actually comprises contributions from two different mechanisms: (1) the dissolution of carbonates previously deposited to the sediments (sea floor CaCO₃ neutralization) and (2) imbalance between weathering and sedimentation (terrestrial CaCO₃ neutralization) [Archer *et al.*, 1997, 1998]. We isolate and quantify the relative contributions to CO₂ sequestration and timescales of these two processes as follows. We start by prescribing a constant weathering flux as before for an open system (0.121 PgC CaCO₃ yr⁻¹) but do not allow ocean DIC or ALK inventories to change as a result of carbonate burial. Instead, we prescribe a rate of removal of DIC and ALK from the ocean floor equal to the weathering flux, except during times of net erosion of deep-sea carbonates, when we subtract the erosion flux (the light grey area in Figure 5e). The resulting flux forcing is shown in Figure 5f. The trajectory of atmospheric CO₂ due to ocean invasion and sea floor CaCO₃ neutralization but excluding the effect of terrestrial CaCO₃ neutralization is shown in Figure 5b. We find that the effects of sea floor and terrestrial carbonate neutralization are approximately equal in magnitude, accounting for the sequestration of 12.4% and 13.7%, respectively, of fossil fuel CO₂ emissions.

[34] We have also determined the characteristic timescales of CO₂ response by log-linear analysis [Sundquist, 1990] (Figure 7), in which the slope of the response curve gives the e -folding time. The sea floor CaCO₃ neutralization response (Figure 7a) is complicated because once emissions have ceased, it takes ~ 1000 years for fossil fuel CO₂ to become fully mixed throughout the ocean. However, from the year ~ 3000 – 3500 onward, CO₂ sequestration by sea floor CaCO₃ neutralization proceeds with a well-defined timescale of ~ 1.7 ka (Figure 7b). This is consistent with a 1500- to 2700-year timescale estimated for a primary alkalinity response in box models [Sundquist, 1990], but about 3 times shorter than the 5–6 ka estimated by Archer *et al.* [1997, 1998]. Differences in model parameterization of bioturbation will affect the rate of exhumation of previously buried carbonates and thus the timescale of CO₂ drawdown. However, we believe that the main reason for the differences in timescale estimates is due to our isolation of the component of ocean chemistry and atmospheric CO₂ changes due to sea floor CaCO₃ neutralization. In contrast, the initial slope of the total CO₂ response reflects both sea floor and terrestrial carbonate neutralization processes operating simultaneously, leading to an estimate for the time constant of the early response inevitably somewhat inter-

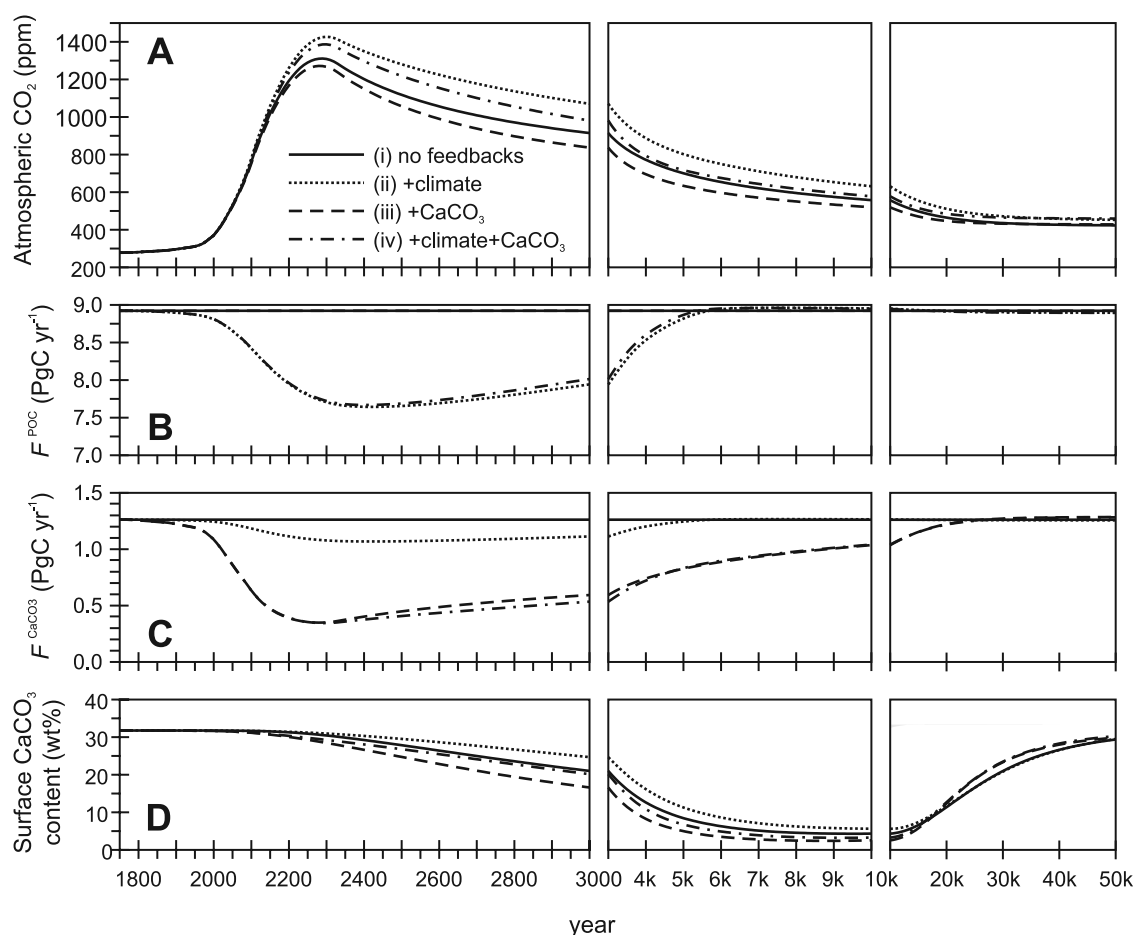


Figure 8. Role of feedbacks in the long-term evolution of atmospheric CO₂. Shown are the results of experiments in which: i, neither climate nor calcification changes with time (solid line); ii, CO₂-climate feedbacks operate (dotted line); iii, calcification responds to atmospheric CO₂ (i.e., the CO₂-calcification feedback) (dashed line); and, iv, both CO₂-calcification and CO₂-climate feedbacks operate (dash-dotted line). (a) Atmospheric CO₂ (ppm). (b) Global particulate organic carbon export (PgC yr⁻¹). (c) Global CaCO₃ export (PgC yr⁻¹). (d) Surface sediment composition (wt% CaCO₃).

mediate between seafloor and terrestrial neutralization responses.

[35] The control on atmospheric CO₂ exerted by terrestrial CaCO₃ neutralization is more gradual. Our estimated timescale of 8.3 ka (Figure 7c) is near identical to previous 3-D ocean-based model analyses (8.2–8.5 ka [Archer *et al.*, 1997, 1998]) and consistent with the 6300–11,800 year “secondary alkalinity response” of Sundquist [1990].

5.2. Importance of Climatic and Calcification Feedbacks With CO₂

[36] Previous analysis of the role of deep-sea sediments in the long-term fate of fossil fuel CO₂ employed off-line tracer-transport marine carbon cycle models in which the ocean circulation was prescribed [e.g., Archer *et al.*, 1997, 1998; Sundquist, 1990]. With a fixed ocean circulation and climatology it is difficult to account for the importance of feedbacks with climate except in a highly parameterized manner [Archer *et al.*, 2004; Archer, 2005]. Because the GENIE-1 model contains a climate component we are able to extend the analysis made in formative earlier studies

[e.g., Archer *et al.*, 1997, 1998; Sundquist, 1990] by now explicitly assessing the impact of major feedbacks between CO₂ and climate on carbonate compensation.

[37] Important feedback may also exist between CO₂ and marine carbonate production. This arises because the continued dissolution of fossil fuel CO₂ in the surface waters of the ocean and associated decrease in ambient carbonate ion concentration [Orr *et al.*, 2005] and pH (termed ocean “acidification” [Caldeira and Wickett, 2003]) may adversely affect the ability of calcifying plankton such as foraminifera and coccolithophores to precipitate CaCO₃ and thus increase the capacity of the surface ocean to absorb CO₂ [Zondervan *et al.*, 2001]. Although there are substantial uncertainties in the likely global response of calcifiers to lower surface pH [Kleypas *et al.*, 2006; Ridgwell *et al.*, 2006], the effect of CO₂-calcification feedback has not previously been considered in long-term (multimillennial scale) analysis of the fate of fossil fuel CO₂.

[38] We therefore now run the calibrated model in each of four permutations of feedbacks operating: (case i) no CO₂-calcification or CO₂-climate feedbacks, (case ii) just

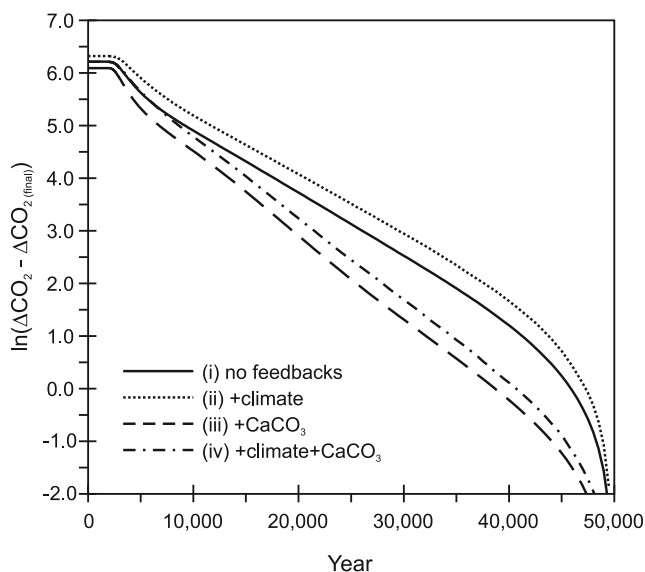


Figure 9. Impact of feedbacks with CO₂ on ocean-sediment buffering. The calculation of $\Delta\text{CO}_2 - \Delta\text{CO}_{2(\text{final})}$ (ppm) is the same as described previously (Figure 7). However, we show only the total contribution of ocean-sediment interactions to CO₂ sequestration, and do not separately resolve seafloor and terrestrial CaCO₃ neutralization components. Shown are the results of experiments in which: i, neither climate nor calcification changes with time (solid line); ii, CO₂-climate feedbacks operate (dotted line); iii, calcification responds to atmospheric CO₂ (i.e., the CO₂-calcification feedback) (dashed line); and iv, both CO₂-calcification and CO₂-climate feedbacks operate (dash-dotted line).

the CO₂-climate feedback, (case iii) just the CO₂-calcification feedback, and (case iv) both CO₂-calcification and CO₂-climate feedbacks. The baseline (“PAC_8”) model configuration used, with the sediments at 36×36 resolution. The same 50 ka spinup is used for all four model experiments. The evolution of atmospheric CO₂ in an open system with seafloor and terrestrial CaCO₃ neutralization processes operating is shown in Figure 8a for the four permutations of feedbacks.

[39] Higher atmospheric CO₂ induces a 5.8°C peak warming of annual mean ocean surface temperature and a weakening of Atlantic meridional overturning from 16.3 to 14.1 Sv. Feedbacks between climatic changes such as these and CO₂ are overall positive [cf. *Friedlingstein et al.*, 2006], resulting in an enhancement of the concentration of CO₂ in the atmosphere compared to the no-feedback case. Associated with the warming-driven stratification of the ocean is a restriction in nutrient supply and thus biological (export) production [*Plattner et al.*, 2001; *Sarmiento et al.*, 1998], with a peak year ~ 2200 reduction of about 16% (Figure 8b). Although stratification affects both particulate organic carbon (POC) and CaCO₃ fluxes (Figure 8c) proportionally, the reduction in POC rather than CaCO₃ rain dominates the net effect on the sediments compared to the no-feedbacks case and carbonate preservation is overall enhanced (Figure 8d). The consequence of this reduction in sedimen-

tary CaCO₃ erosion is a weaker buffering of atmospheric CO₂. This can be seen in the tendency for the CO₂ difference between the no feedbacks and CO₂-climate feedbacks cases to increase through the current millennium (i.e., to year 3000) (Figure 8a), reflecting the weaker contribution from seafloor carbonate neutralization to CO₂ sequestration. The effect of adding CO₂-climate feedback is to extend the timescale (the slightly less steep initial slope) and reduce the overall contribution (the less extreme minimum in wt% CaCO₃ in Figure 8d) of seafloor CaCO₃ neutralization as shown in Figure 9.

[40] Feedback between CO₂ and calcification is overall negative, enhancing fossil fuel CO₂ sequestration. In the GENIE-1 model, a substantial reduction in CaCO₃ export occurs in response to ocean surface acidification [*Ridgwell et al.*, 2006] (Figure 8c) resulting in a pronounced acceleration of both seafloor and terrestrial CaCO₃ neutralization processes, indicated by the steepening of initial and long-term slopes in Figure 9. One caveat to this analysis it that we have not included a possible dependence of carbonate rain fluxes on the efficiency of organic matter transport into the deep ocean [*Armstrong et al.*, 2002; *Klaas and Archer*, 2002], which would reduce our predicted impact of CO₂-calcification feedback on the sediments [*Ridgwell*, 2003].

5.3. Sensitivity of Future CO₂ Predictions to Model Configuration

[41] All numerical models of climatic and/or biogeochemical processes have an inherent uncertainty associated with their parameterization and configuration (e.g., resolution). Although this has important implications for the interpretation of model predictions, the uncertainty associated with model parameterization is much less readily characterized than that associated with parameter values. To assess the sensitivity of our CO₂ predictions to model configuration we have contrasted the CO₂ responses of the different calibrations of GENIE-1. The results (Table 1) demonstrate that the effect of subgridding the SEDGEM sediments module at 72×72 and consequential subtle redistribution of CaCO₃ preservation (compare Figure 3d with Figure 4e) has relatively little affect on the trajectory of atmospheric CO₂ compared to using the same parameter set but with SEDGEM at 36×36 . A larger difference is observed if the “PAC_10” parameter set is used at 36×36 resolution; year CO₂ is 3 ppm lower and declines much quicker with time than under “PAC_8”, reaching 30 ppm lower by the year 10000. This arises both owing to a larger initial erodable CaCO₃ inventory (38.4 wt%) as well as a greater weathering throughput ($0.153 \text{ PgC yr}^{-1}$), enhancing seafloor and terrestrial carbonate neutralization mechanisms, respectively. The importance of ocean-sediment interactions are greatest under “PA_8” because of the larger yet initial CaCO₃ inventory (40.3 wt%) and weathering throughput ($0.179 \text{ PgC yr}^{-1}$). However, even the 41 ppm year 10,000 difference between “PAC_8” and “PA_8” predictions is small compared to overall 365 ppm importance of ocean-sediment interactions (Figure 5).

[42] It is notable that across the four experiments, year 50,000 CO₂ is virtually independent of the model configuration, supporting our assumption that this point in time is

reasonably close to steady state. The uniform final CO₂ value represents the titration of fossil fuel CO₂ with CaCO₃ to the point at which the pre-industrial saturation state of the ocean is restored. The subsequent fate of this residual CO₂ would be drawdown by silicate weathering feedback [Ridgwell and Zeebe, 2005].

6. Conclusions

[43] The inclusion of a deep-sea sediment module in GENIE-1 has allowed us to make innovative use of available global sedimentary data via an ensemble Kalman filter. This is the first time that sediment composition data has been used in inverse modeling and our results demonstrate that it provides an improved constraint on the modern marine carbon cycling compared to assimilation of ocean geochemical observations alone. The calibrated model successfully captures most of the observed features of the global distribution of wt% CaCO₃ in marine sediments while our 0.121 PgC yr⁻¹ estimate for the deep-sea carbonate sink is in line with previous model and data-based estimates.

[44] We have employed the calibrated GENIE-1 model to revisit the long-term fate of fossil fuel CO₂ and isolated the two components of CO₂ sequestration arising from the phenomenon of carbonate compensation, changes in ocean chemistry due to the dissolution of carbonates previously deposited to the sediments (seafloor CaCO₃ neutralization) and imbalances between weathering and sedimentation (terrestrial CaCO₃ neutralization). By doing this we find that seafloor CaCO₃ neutralization acts with a faster response time (1.7 ka) than previously estimated, making this process more important to future millennial-scale change than was assumed. In contrast, the adjustment of ocean chemistry to rectify imbalances between weathering and carbonate burial is characterized by a much longer timescale of 8.3 ka. We have also carried out the first explicit analysis of the coupled atmosphere-ocean-sediment plus climate system and found that decreased particulate organic carbon export due to surface warming and increased ocean stratification weakens seafloor CaCO₃ neutralization. This represents a new positive feedback on millennial-scale future climate change.

[45] Our calibrated representation of atmosphere-ocean-sediment carbon cycling within a 3-D ocean circulation based climate model achieves >1000 years per (2.4 GHz) CPU hour on a desktop PC. The GENIE-1 model thus represents a powerful alternative to box models and GCM trained simulators in carrying sensitivity analyses and extended simulations of the long-term fate of fossil fuel and efficiency of CO₂ sequestration by deep injection.

[46] **Acknowledgments.** A. R. acknowledges a University Research Fellowship from the Royal Society, as well as support via a Canada Research Chair and from the Canadian Foundation for Climate and Atmospheric Sciences. Computer facilities for the EnKF calculations were provided by JAMSTEC.

References

Andersson, J. H., J. W. M. Wijsman, P. M. J. Herman, J. J. Middelburg, K. Soetaert, and C. Heip (2004), Respiration patterns in the deep ocean, *Geophys. Res. Lett.*, *31*, L03304, doi:10.1029/2003GL018756.

Annan, J. D., J. C. Hargreaves, N. R. Edwards, and R. Marsh (2005), Parameter estimation in an intermediate complexity Earth system model using an ensemble Kalman filter, *Ocean Modell.*, *8*, 135–154.

Archer, D. (1991), Modeling the calcite lysocline, *J. Geophys. Res.*, *96*, 17,037–17,050.

Archer, D. (1996), A data-driven model of the global calcite lysocline, *Global Biogeochem. Cycles*, *10*, 511–526.

Archer, D. (2005), Fate of fossil fuel CO₂ in geologic time, *J. Geophys. Res.*, *110*, C09S05, doi:10.1029/2004JC002625.

Archer, D., S. Emerson, and C. Reimers (1989), Dissolution of calcite in deep-sea sediments: pH and O₂ microelectrode results, *Geochim. Cosmochim. Acta*, *53*, 2831–2845.

Archer, D., H. Khesghi, and E. Maier-Reimer (1997), Multiple timescales for neutralization of fossil fuel CO₂, *Geophys. Res. Lett.*, *24*, 405–408.

Archer, D., H. Khesghi, and E. Maier-Reimer (1998), Dynamics of fossil fuel CO₂ neutralization by marine CaCO₃, *Global Biogeochem. Cycles*, *12*, 259–276.

Archer, D., A. Winguth, D. Lea, and N. Mahowald (2000), What caused the glacial/interglacial atmospheric pCO₂ cycles?, *Rev. Geophys.*, *38*, 159–189.

Archer, D. E., J. L. Morford, and S. R. Emerson (2002), A model of suboxic sedimentary diagenesis suitable for automatic tuning and gridded global domains, *Global Biogeochem. Cycles*, *16*(1), 1017, doi:10.1029/2000GB001288.

Archer, D., et al. (2004), The importance of ocean temperature to global biogeochemistry, *Earth Planet. Sci. Lett.*, *222*, 333–348.

Armstrong, R. A., C. Lee, J. I. Hedges, S. Honjo, and S. G. Wakeham (2002), A new, mechanistic model for organic carbon fluxes in the ocean: Based on the quantitative association of POC with ballast minerals, *Deep Sea Res., Part II*, *49*, 219–236.

Broecker, W. S., and T.-H. Peng (1987), The role of CaCO₃ compensation in the glacial to interglacial atmospheric CO₂ change, *Global Biogeochem. Cycles*, *1*, 15–29.

Caldeira, K., and M. E. Wickett (2003), Anthropogenic carbon and ocean pH, *Nature*, *425*, 365.

Edwards, N. R., and R. Marsh (2005), Uncertainties due to transport-parameter sensitivity in an efficient 3-D ocean-climate model, *Clim. Dyn.*, *24*, 415–433.

Emerson, S., and M. Bender (1981), Carbon fluxes at the sediment-water interface of the deep-sea: Calcium carbonate preservation, *J. Mar. Res.*, *39*, 139–162.

Enting, I. G., T. M. L. Wigley, and M. Heimann (1994), Future emissions and concentrations of carbon dioxide: Key ocean/atmosphere/land analyses, *Tech. Pap. 31*, Div. of Atmos. Res., Commonw. Sci. and Ind. Res. Org., Aspendale, Victoria, Australia.

Feely, R. A., et al. (2004), Impact of anthropogenic CO₂ on the CaCO₃ system in the oceans, *Science*, *305*, 362–366.

Friedlingstein, P. (2006), Climate-carbon cycle feedback analysis, results from the C4MIP model intercomparison, *J. Clim.*, *19*, 3337–3353.

Gehlen, M., L. Bopp, N. Emprin, O. Aumont, C. Heinze, and O. Ragueneau (2006), Reconciling surface ocean productivity, export fluxes and sediment composition in a global biogeochemical ocean model, *Biogeosciences*, *3*, 521–537.

Gibbs, M. T., G. J. S. Bluth, P. J. Fawcett, and L. R. Kump (1999), Global chemical erosion over the last 250 My: variations due to changes in paleogeography, paleoclimate, and paleogeology, *Am. J. Sci.*, *299*, 611–651.

Hargreaves, J. C., J. D. Annan, N. R. Edwards, and R. Marsh (2004), Climate forecasting using an intermediate complexity Earth system model and the Ensemble Kalman Filter, *Clim. Dyn.*, *23*, 745–760.

Heinze, C. (2001), Towards the time dependent modeling of sediment core data on a global basis, *Geophys. Res. Lett.*, *28*, 4211–4214.

Heinze, C., E. Maier-Reimer, A. M. E. Winguth, and D. Archer (1999), A global oceanic sediment model for long-term climate studies, *Global Biogeochem. Cycles*, *13*, 221–250.

Hotinski, R. M., L. R. Kump, and R. G. Najjar (2000), Opening Pandora's Box: The impact of open system modeling on interpretations of anoxia, *Paleoceanography*, *15*, 267–279.

Jin, X., N. Gruber, J. Dunne, J. L. Sarmiento, and R. A. Armstrong (2006), Diagnosing the contribution of phytoplankton functional groups to the production and export of POC, CaCO₃ and opal from global nutrient and alkalinity distributions, *Global Biogeochem. Cycles*, *20*, GB2015, doi:10.1029/2005GB002532.

Keeling, C. D., and T. P. Whorf (2004), Atmospheric CO₂ records from sites in the SIO air sampling network, in *Trends: A Compendium of Data on Global Change*, Carbon Dioxide Inf. Anal. Cent., Oak Ridge Natl. Lab., U.S. Dep. of Energy, Oak Ridge, Tenn. (Available at <http://cdiac.esd.ornl.gov/trends/co2/sio-mlo.htm>)

- Klaas, C., and D. E. Archer (2002), Association of sinking organic matter with various types of mineral ballast in the deep sea: Implications for the rain ratio, *Global Biogeochem. Cycles*, *16*(4), 1116, doi:10.1029/2001GB001765.
- Kleypas, J. A., R. A. Feely, V. J. Fabry, C. Langdon, C. L. Sabine, and L. L. Robbins (2006), Impacts of ocean acidification on coral reefs and other marine calcifiers: A guide for future research, workshop report, 88 pp., Natl. Sci. Found., Washington, D. C.
- Lenton, T. M. (2000), Land and ocean carbon cycle feedback effects on global warming in a simple Earth system model, *Tellus, Ser. B*, *52*, 1159–1188.
- Lenton, T. M., M. S. Williamson, N. R. Edwards, R. J. Marsh, A. R. Price, A. J. Ridgwell, J. G. Shepherd, S. J. Cox, and GENIE team (2006), Millennial timescale carbon cycle and climate change in an efficient Earth system model, *Clim. Dyn.*, *26*(7-8), 687–711, doi:10.1007/s00382-006-0109-9.
- Lutz, M., R. Dunbar, and K. Caldeira (2002), Regional variability in the vertical flux of particulate organic carbon in the ocean interior, *Global Biogeochem. Cycles*, *16*(3), 1037, doi:10.1029/2000GB001383.
- Milliman, J. D., and A. W. Droxler (1996), Neritic and pelagic carbonate sedimentation in the marine environment: Ignorance is not bliss, *Geol. Rundsch.*, *85*, 496–504.
- Munhoven, G. (2002), Glacial-interglacial changes of continental weathering: Estimates of the related CO₂ and HCO₃⁻ flux variations and their uncertainties, *Global Planet. Change*, *33*, 155–176.
- Orr, J. C., et al. (2005), Anthropogenic ocean acidification over the twenty-first century and its impact on calcifying organisms, *Nature*, *437*, 681–686.
- Oxburgh, R., and W. S. Broecker (1993), Pacific carbonate dissolution revisited, *Palaeogeogr. Palaeoclimatol. Palaeoecol.*, *103*, 31–39.
- Plattner, G. K., F. Joos, T. F. Stocker, and O. Marchal (2001), Feedback mechanisms and sensitivities of ocean carbon uptake under global warming, *Tellus, Ser. B*, *53*, 564–592.
- Ridgwell, A. J. (2001), Glacial-interglacial perturbations in the global carbon cycle, Ph.D. thesis, Univ. of East Anglia at Norwich, Norwich, U.K. (Available at http://andy.seao2.org/pubs/ridgwell_2001.pdf)
- Ridgwell, A. J. (2003), An end to the “rain ratio” reign?, *Geochem. Geophys. Geosyst.*, *4*(6), 1051, doi:10.1029/2003GC000512.
- Ridgwell, A. (2006), Application of sediment core modelling to understanding climates of the past: An example from glacial-interglacial changes in Southern Ocean silica cycling, *Clim. Past Disc.*, *2*, 1371–1386.
- Ridgwell, A., and R. E. Zeebe (2005), The role of the global carbonate cycle in the regulation and evolution of the Earth system, *Earth Planet. Sci. Lett.*, *234*, 299.
- Ridgwell, A., I. Zondervan, J. Hargreaves, J. Bijma, and T. Lenton (2006), Significant long-term increase of fossil fuel CO₂ uptake from reduced marine calcification, *Biogeosci. Disc.*, *3*, 1763–1780.
- Ridgwell, A., J. Hargreaves, N. Edwards, J. Annan, T. Lenton, R. Marsh, A. Yool, and A. Watson (2007), Marine geochemical data assimilation in an efficient Earth system model of global biogeochemical cycling, *Biogeosciences*, *4*, 87–104.
- Sarmiento, J. L., T. M. C. Hughes, R. J. Stouffer, and S. Manabe (1998), Simulated response of the ocean carbon cycle to anthropogenic climate warming, *Nature*, *393*, 245–249.
- Sitch, S., V. Brovkin, W. von Bloh, D. van Vuuren, B. Eickhout, and A. Ganopolski (2005), Impacts of future land cover changes on atmospheric CO₂ and climate, *Global Biogeochem. Cycles*, *19*, GB2013, doi:10.1029/2004GB002311.
- Stuiver, M., and H. A. Polach (1977), Reporting of ¹⁴C Data, *Radiocarbon*, *19*, 355–363.
- Sundquist, E. T. (1990), Influence of deep-sea benthic processes on atmospheric CO₂, *Philos. Trans. R. Soc., Ser. A*, *331*, 155–156.
- Vecsei, A. (2004), A new estimate of global reefal carbonate production including the fore-reefs, *Global Planet. Change*, *43*, 1–18.
- Zondervan, I., R. E. Zeebe, B. Rost, and U. Riebesell (2001), Decreasing marine biogenic calcification: A negative feedback on rising atmospheric pCO₂, *Global Biogeochem. Cycles*, *15*, 507–516.

J. C. Hargreaves, Frontier Research Center for Global Change, 3173-25 Showa-machi, Kanazawa-ku, Yokohama, Kanagawa 236-0001, Japan.

A. Ridgwell, School of Geographical Sciences, University of Bristol, University Road, Bristol BS8 1SS, UK. (andy@seao2.org)